

THE IMPROVEMENT OF THE SEISMIC VULNERABILITY OF STEEL STORAGE TANKS WITH SLIDING ISOLATORS

Riccardo R. Milanese¹, Giammaria Gabbianelli², Emanuele Gandelli³,
Paolo Dubini⁴, Roberto Nascimbene⁵

¹ European Centre for Training and Research in Earthquake Engineering (EUCENTRE), Pavia, Italy.

riccardo.milanese@eucentre.it

² Department of Civil Engineering and Architecture, University of Pavia, Pavia, Italy.

³ DICATAM, University of Brescia, Brescia, Italy.

⁴ European Centre for Training and Research in Earthquake Engineering (EUCENTRE), Pavia, Italy.

⁵ University School for Advanced Studies IUSS Pavia, Pavia, Italy.

Abstract: *The improvement of the seismic performance of industrial plants represents a fundamental need to guarantee the environmental and life safety of the area surrounding the plant. The industrial facilities that are working, for example, in the chemical or the petrochemical fields, usually have large steel storage tanks, which recent post-seismic surveys have observed can suffer several damages such as the elephant-foot-buckling, the uplift or the complete instability with the overturning of the structure. Such structural damage can cause the plant's shutdown, reducing the local infrastructure's resilience, or even large dispersions of the content in the environment, with adverse effects on human safety and the ecosystem.*

Due to the uncertainties related to the estimation of the mechanical properties of filled tanks and related seismic loads (i.e., dynamic overpressures generated by the content), conventional design approaches may lead to unsafe or, on the contrary, oversized solutions.

The base isolation through Curved Surface Sliders isolators (CSSs) has been adopted in different structures, and the use of such a system for steel storage tank applications is not wide to the difficulties in the design process.

The present paper discusses a study on the influence of base isolation with CSSs to highlight the valuable advantages in terms of the improvement of the seismic vulnerability of steel storage tanks.

Furthermore, the initial peak of friction force at CSSs' motions breakaway modifies the overall response of the isolated system. Within this framework in this study, a parametric investigation through a numerical model developed in OpenSees FEM code is carried out to compare the effect of the breakaway and different materials in the CSSs on isolated tanks providing useful insights for the selection of the most suitable device.

1. Introduction

Recent earthquakes, like the one in Emilia-Romagna, Italy, in 2012, emphasized the need for improvement of the seismic design in industrial structures. Observations after these earthquakes showed significant damage and collapses in precast structures, storage tanks, and steel storage pallet racks. Steel storage tanks vary based on factors such as their shape, roof type, base restraints, interaction with the foundation/soil, and their contents. Among these, tanks with liquid content and interactions with the foundation/soil are particularly

important due to their size. Common damage in steel storage tanks includes sloshing effects, elephant-foot-buckling of tank walls, and ruptures in attached piping systems. These failures are often due to standardized tank production, rather than a lack of seismic design codes. Properly designing these structures is crucial because tank collapses can result in human casualties and environmental pollution. Steel storage tanks are often used for storing hazardous materials, making their operational stability essential during and after earthquakes. Additionally, these tanks can be installed within industrial buildings, affecting the behavior of the overall structure.

To ensure seismic safety, researchers have developed simplified models and detailed finite element models to simulate the seismic response of tanks. Some focus on decoupling the impulsive and convective components of motion, while others explicitly consider fluid-structure interaction. For new tanks, seismic design can include strengthening the anchorage system and increasing wall thickness, but this can be costly. Anchored tanks are susceptible to large overturning moments due to hydrodynamic pressures, while unanchored tanks may experience partial base uplifting, causing buckling failures. To achieve safety standards economically, alternative approaches like base isolation systems have been explored.

Researchers have investigated various base isolation methods, including rubber bearings, friction pendulum systems, and other passive control systems, to improve seismic performance in tanks. These methods have been found effective in reducing structural damage and maintaining operational functionality. In this study, the authors investigate the influence of different Curved Surface Slider (CSS) isolators on steel tanks using Multiple-Stripe Analysis. CSS isolators offer advantages such as high load-bearing capacity, compact dimensions, independence of natural oscillation periods from superstructure mass, and minimal torsional effects in asymmetric superstructures. A CSS comprises two concave sliding plates with or without identical curvature, polymer pads, and a central pivot element. The radius of curvature of the sliding surfaces (R) determines the isolation period and provides recentering force (F_r) proportional to displacement. Seismic energy dissipation (damping) relies on the friction force (F_f), resulting in an ideal bilinear force-displacement response.

$$F = F_r + F_f = \left(\frac{N}{R}\right) \cdot d + (\mu \cdot N) \cdot \text{sign}(V) \quad (1)$$

The Equation (1) mentions μ as the instantaneous friction coefficient on the sliding surfaces and $\text{sign}(V)$ as the signum function of the sliding velocity (V). Additionally, (N / R) and (μN) represent the restoring stiffness (k_r) and characteristic strength (F_0) of the isolator, respectively. The initial stiffness (k_i) of the CSS during the pre-sliding phase is notably high, typically twice the restoring stiffness, i.e., $k_i=100 k_r$ (Naeim and Kelly 1999).

According to Equation (2), the friction coefficient (μ) of the sliding pad, typically made of materials like PTFE or UHMWPE in dry or lubricated conditions, plays a significant role in the CSS's hysteresis behavior. This is influenced by various factors, including changes in the average contact pressure (e.g., due to rocking motions) and rising temperatures caused by frictional heating phenomena (Constantinou et al., 1990; Quaglini et al., 2019). Most importantly, the friction coefficient (μ) is primarily controlled by the instantaneous sliding velocity (Constantinou et al., 1990).

$$\mu = \mu_{HV} - (\mu_{HV} - \mu_{LV}) \cdot e^{(-\alpha V)} \quad (2)$$

The coefficient of friction, denoted as μ_{HV} for very high velocities ($V>100\text{mm/s}$) and μ_{LV} for very low velocities ($V<1\text{mm/s}$), is essential for understanding the behavior of the system. The parameter α regulates the transition between these velocity regimes. However, this formulation neglects the initial peak of the friction coefficient (μ_B) at motion breakaway (Gandelli and Quaglini, 2020; Gandelli et al., 2020). As a drawback, the breakaway can substantially increase both the base shear and the accelerations transmitted to the superstructure, leading to higher lateral drifts. Notably, these effects are negligible for low-friction materials ($\mu=0.01\div 0.03$) but become important for medium ($\mu=0.03\div 0.08$) and high-friction materials ($\mu=0.05\div 0.13$) when the ratio between the breakaway and low-velocity friction coefficients exceeds 2.5 ($\mu_B / (\mu_{LV}>2.5)$).

With this in mind, the current research investigates the seismic vulnerability of steel storage tanks through a parametric study conducted in the OpenSees FEM code (McKenna et al., 2006). It involves various combinations of tanks with CSSs, where the isolation system is simulated using the recently developed "BV element", i.e., Breakaway and Velocity dependent formulation (Gandelli et al., 2019). This BV element accurately captures the initial transition from sticking to slow sliding motion (from μ_B to μ_{LV}) and the subsequent

transition to high velocities (from μ_{LV} to μ_{HV}), as shown in Figure 1-c. The study herein presented is detailed in Gabbianelli et al. (2023).

The study herein presented summarizes the work discussed by Gabbianelli et al. (2023).

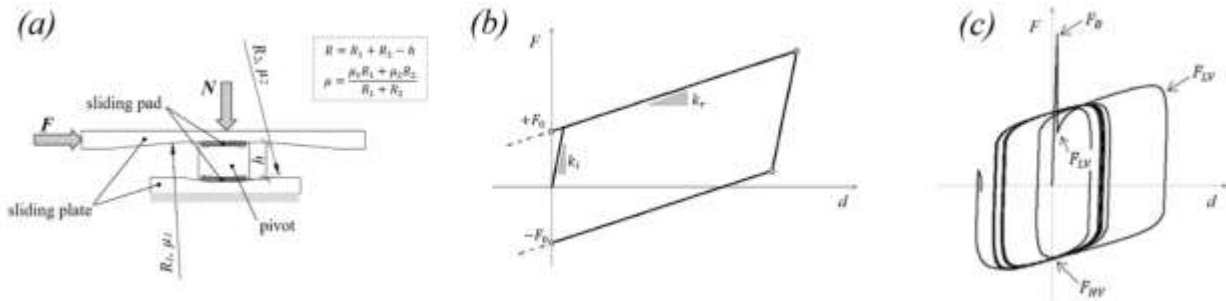


Figure 1 The CSS isolator: (a) main components; (b) idealised bilinear force-displacement response; (c) example of actual cyclic response, accounting both velocity and breakaway effects, calculated through the novel BV element (Gabbianelli et al., 2023).

2. Description of the model and the analyses performed

2.1. Isolation systems

In the present study, the use of CSS isolators placed at the tank base, employing the innovative BV element integrated into the OpenSees FEM code (McKenna et al., 2006). Three friction categories have been explored: low friction (LF), medium friction (MF), and high friction (HF). Table 2 lists the respective low-velocity (μ_{LV}), high-velocity (μ_{HV}), and breakaway (μ_B) friction coefficients. These categories correspond to typical sliding pad materials at mild ambient temperatures (10-30°C): lubricated PTFE and UHMWPE against polished steel (LF), unlubricated PTFE and UHMWPE (MF), and filled PTFE (HF) (Quaglino et al., 2012).

To ensure consistency, a μ_{HV} / μ_{LV} ratio of 2.5 for all friction cases has been assumed, and the transition rate parameter α from low-velocity to high-velocity friction to $\alpha=0.0055$ s/mm has been set, as determined by Cardone et al. (2015). For each friction category, three breakaway scenarios based on μ_B / μ_{LV} ratios have been considered: no breakaway for $\mu_B / \mu_{LV} = 1$, intermediate breakaway for $\mu_B / \mu_{LV} = 2$, and high breakaway for $\mu_B / \mu_{LV} = 4$. These scenarios cover a range of conditions, from typical structural analysis program models ($\mu_B / \mu_{LV} = 1$) to situations with lubricated materials ($\mu_B / \mu_{LV} = 2$) and challenging conditions due to low temperature, poor maintenance, mounting issues, or permanent surface setting ($\mu_B / \mu_{LV} = 4$) (Constantinou et al., 1990; Pavese et al., 2019).

All CSS isolators in this study share an effective radius of curvature of $R=3000$ mm, resulting in an undamped isolation period of $T_{iso}=2\pi\sqrt{(R_{eff}/g)}=3.48$ s. This period falls within the common range of $T_{iso}=2\div 5$ s, providing suitable protection for the tanks. Other CSSs will be studied in future investigations.

Table 1. Design friction parameters of the sliding isolators considered in the present study.

Friction class	Representative case	Friction coefficient (μ_{LV}, μ_{HV})	Breakaway class	Breakaway friction μ_B	Isolation ID
LF	lubricated PTFE / UHMWPE	(0.01,0.025)	$\mu_B/\mu_{LV} = 1$	0.01	Isol-1
			$\mu_B/\mu_{LV} = 2$	0.02	Isol-2
			$\mu_B/\mu_{LV} = 4$	0.04	Isol-3
MF	unlubricated PTFE / UHMWPE	(0.03,0.075)	$\mu_B/\mu_{LV} = 1$	0.03	Isol-4
			$\mu_B/\mu_{LV} = 2$	0.06	Isol-5
			$\mu_B/\mu_{LV} = 4$	0.12	Isol-6
HF	filled PTFE	(0.05,0.125)	$\mu_B/\mu_{LV} = 1$	0.05	Isol-7
			$\mu_B/\mu_{LV} = 2$	0.10	Isol-8
			$\mu_B/\mu_{LV} = 4$	0.20	Isol-9

2.2. Model assumption for steel tanks

In this study, numerical models have been used to simulate the seismic response of cylindrical steel tanks for liquid storage that are isolated using CSSs. The Malhotra model (Malhotra, 1997; 2000) has been adopted to simulate the tank's response above the isolation layer. This model accounts for the hydrodynamic interaction between the fluid and the tank, avoiding the need for computationally intensive three-dimensional finite element models with Arbitrary Lagrangian-Eulerian (ALE) formulation (Takashi, 1994). The Malhotra model is commonly used in practice and it is included in European standards (EN 1998-4, 2006).

In this computational framework, dynamic analysis is carried out using a generalized single-degree-of-freedom system approach. Each degree of freedom represents a distinct vibration mode of the tank-fluid system. The response has been calculated for each mode independently and then combine them using a chosen modal combination rule.

Further info about the model adopted (sketched in Figure 2), the actions governing the design of the tanks and the dimensions of the tanks taken into account are reported by Gabbianelli *et al.* (2023). Three sites (low-, medium- and high-seismicity) have been taken into account, for each location, ten different tanks were designed, increasing the radius of the tank in order to obtain a sufficient variability of the tank configurations.

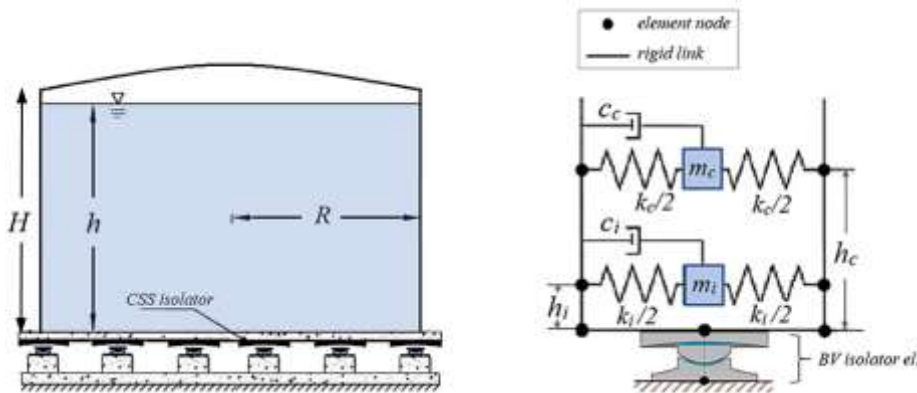


Figure 2 Steel storage tank implementing CSS isolators: physical layout (left), and refined numerical model proposed in this study (right) [Gandelli *et al.*, 2022].

2.3. Description of the analyses conducted through PSHA

To conduct nonlinear dynamic analyses effectively, it is crucial to use ground motion records that align with the seismic hazard of the study site. Therefore, a probabilistic seismic hazard analysis (PSHA) has been conducted to determine the earthquake rate exceeding the selected ground-motion intensity measure (IM) threshold at the site (Cornell, 1968). In recent years, PSHA has often employed peak ground acceleration (PGA) or spectral acceleration (SA) as the IM. In the present study SA has been used.

The PSHA have been conducted for three distinct Italian sites in Italy: Sannazzaro de' Burgondi (PV), Fiorenzuola d'Arda (PC), and Vibo Valentia (VV), representing low, medium, and high seismic intensity sites, respectively. These sites were categorized as having soil type C, following Eurocode 8 (EN 1998-1, 2011) and NTC18 (NTC18, 2018) classification standards.

Regarding the nonlinear dynamic analysis methodology, the Multiple-Stripe Analysis (MSA) approach has been adopted, as suggested by Baker (2015). The MSA method requires selecting a set of ground motions for each return period (RP) and defining a target spectrum to match within the ground-motion records, further information about the ground motion selection is reported in Gabbianelli *et al.* (2023). As an example, Figure 3, illustrates the UHS, CS(AvgSA), median spectrum \pm standard deviation and single spectra of the selected records, for each limit state and for the medium-seismicity (Fiorenzuola d'Arda) site.

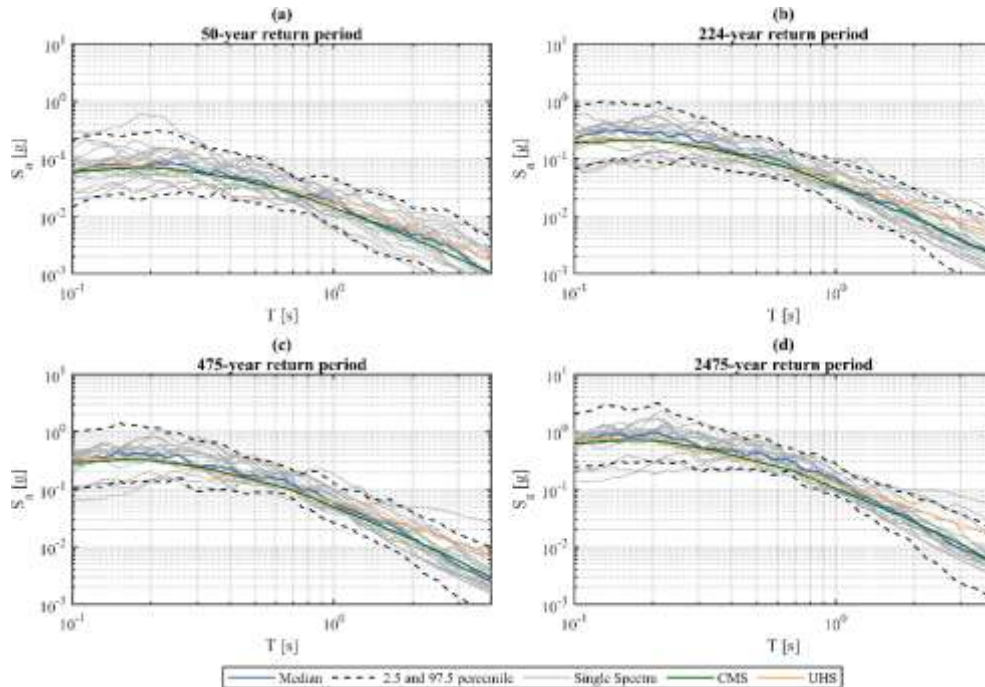


Figure 3 UHS, CS(AvgSA), median spectrum, median spectrum plus standard deviation and single spectra for Fiorenzuola, Italy.

3. Damage states for base isolated steel tanks

The typical structural damages observed in tank systems have been documented through field observations after seismic events and past experimental and numerical studies, as cited in references (Caprinuzzi et al., 2020; Merino Vela et al., 2019; Bakalis and Karomanos, 2021; Merino Vela et al., 2018). These damages include issues like sloshing of stored fluid, yielding or failure of anchor systems, and elephant's foot buckling (EFB) of tank walls. Various authors have addressed the definition of limit states related to steel tanks subjected to seismic loads, including i.e. Merino Vela et al. (2019). In particular, Brunesi et al. (2015) and Merino Vela et al. (2019) have highlighted that tanks are commonly susceptible to damage due to convective waves in the stored fluid (sloshing), yielding or failure of anchor systems, and EFB of tank walls. Merino Vela et al. (2019) proposed limit state thresholds for buckling-dominated modes, sloshing-related damage, and anchor system failure. Seismic vulnerability assessment typically considers four limit states: yielding of the anchor system; failure of anchor bolts; development of EFB mechanism in tank walls; sloshing wave height exceeding the freeboard height.

In this study, the anchor system limit states has not been taken into account since a design of the CSSs' anchor system has been assumed. However, two additional limit states related to the overall seismic behavior of the tanks have been considered: development of EFB mechanism in tank walls; uplift of tanks relative to the foundation, assuming no tie-down systems are installed; overall instability of the tank leading to complete overturning.

The limit state corresponding to EFB is typically assessed by converting recorded force time-histories into stress time-histories and comparing the results with a critical stress buckling limit. The stresses have been computed according to EC8 Part 4 (2006), EC6 Part 1-3 (2007); meanwhile the uplift and the overall instability (overturning) have been defined through the computation of the anchorage ratio J-factor accordingly to the API Standard 650 (2020). Additional info are available in Gabbianelli et al. (2023).

4. Outcomes of the study

The frictional properties of CSS isolators significantly impact the dynamic response of base-isolated tanks, as illustrated in Figure 4. This figure compares base shear versus displacement time histories for all considered isolation systems ("Isol-1÷9") placed at the base of the same tank subjected to one of the selected ground motions for a high seismicity site (Vibo Valentia) with a return period of 2475 years. The different damping capacities provided by the CSSs' friction classes are evident. Specifically, high friction (HF) isolators ("Isol-

7÷9") exhibit the most significant base shear reduction and reduced maximum displacement compared to low friction (LF) isolators ("Isol-1÷3"), where displacement is maximized, and base shear is minimized. The influence of breakaway friction (μ_B) can also be observed, with, for instance, a significant peak of base shear (14 MN) predicted at motion breakaway for "Isol-9." Although μ_B is lower for other CSS configurations, it can lead to potential underestimations of forces transmitted to the anchoring system. For example, "Isol-7," which shares low (μ_{LV}) and high (μ_{HV}) velocity friction coefficients with "Isol-9" but neglects breakaway ($\mu_B = 0$), results in a reduced maximum base shear (11 MN, i.e., -21%). This trend is further confirmed by Figure 5a, which displays the base shear (median, 25th, and 75th percentile values) of different isolated tanks ("Isol-1÷9") exposed to ground motion records selected for a return period of 975 years (Life Safety Limit State) for medium seismicity site.

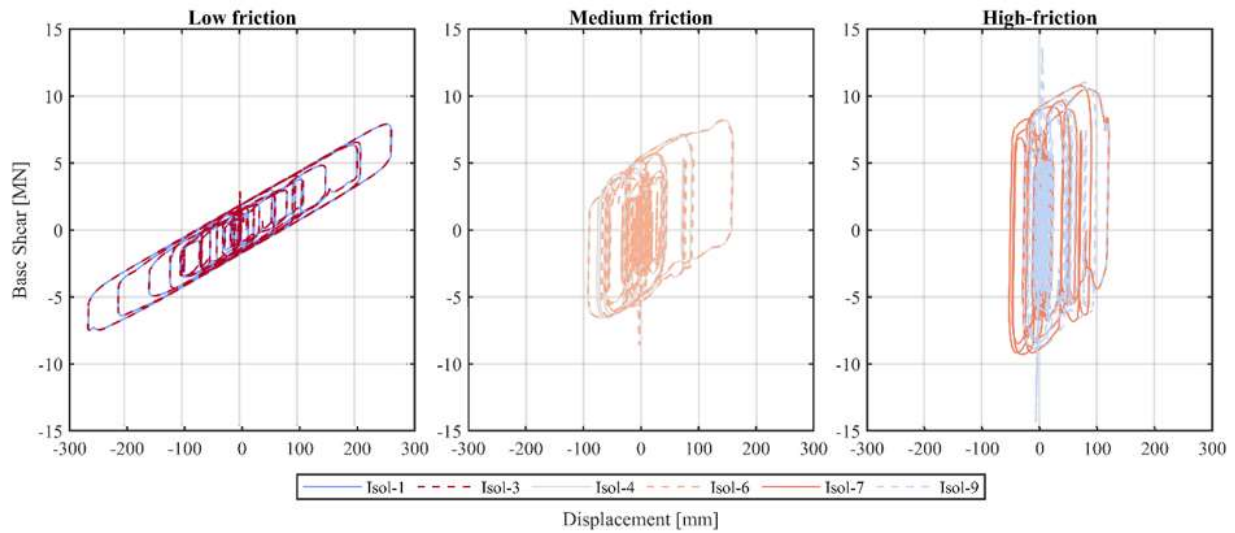


Figure 4 Hysteretic loops calculated for the different CSS layouts protecting Tank #5 when subjected to one of the ground motions selected for the site of Vibo Valentia and a return period of 2475 years (Gabbianelli et al., 2023).

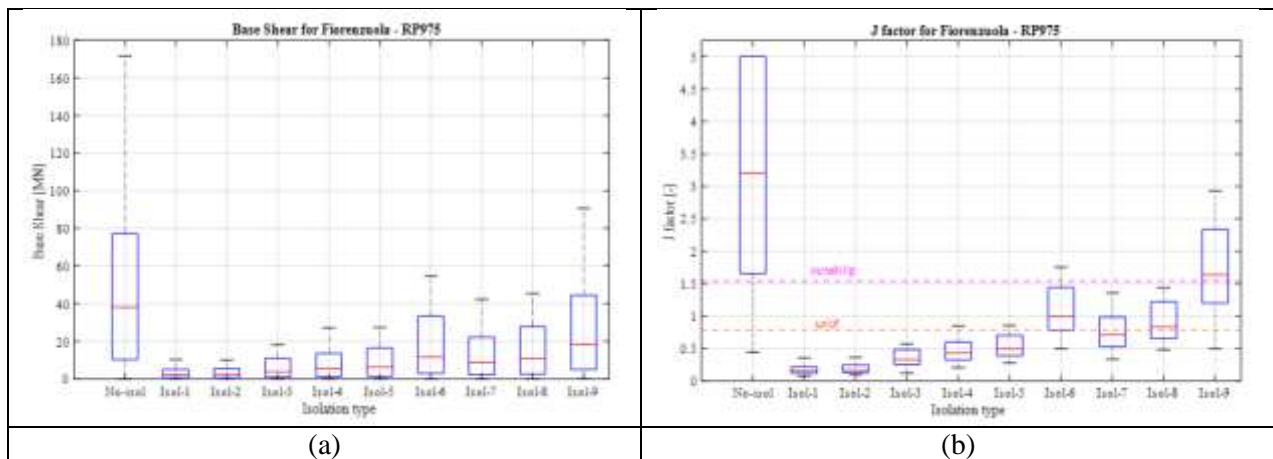


Figure 5 Comparison of maximum base shear (a) and J-factor (b) for all tank configurations considered for Fiorenzuola site (mid seismicity) when subjected to the seismic scenario with RP of 975 years. The red line represents the median value, whereas the bottom and top edges of the box are the 25th and 75th percentiles (Gabbianelli et al., 2023).

Given that "elephant-foot-buckling" (EFB) issues are generally mitigated by any form of isolation layer (see Table 2), the primary focus of the parametric study is on comparing various "tank plus CSS" combinations concerning maximum base shear, uplift, and instability (overturning). Despite the simplifications in the adopted numerical approach, such as the absence of hold-down systems for the sliding isolators, these comparisons offer valuable insights for the preliminary design of tanks implementing CSS devices.

Table 2 Number of occurrences for the three different limit states (over a total of 3000 events) (Gabbianelli et al., 2023)

Sannazzaro (Low seismicity site)						
	EFB		Uplift		Unstable	
	[-]	[%]	[-]	[%]	[-]	[%]
No-isol	791	26.4	1535	51.2	996	33.2
Isol-1	0	0.0	0	0.0	0	0.0
Isol-2	0	0.0	0	0.0	0	0.0
Isol-3	0	0.0	0	0.0	0	0.0
Isol-4	0	0.0	18	0.6	0	0.0
Isol-5	0	0.0	629	21.0	0	0.0
Isol-6	0	0.0	1619	54.0	545	18.2
Isol-7	0	0.0	973	32.4	0	0.0
Isol-8	0	0.0	1466	48.9	133	4.4
Isol-9	321	10.7	1622	54.1	967	32.2
Fiorenzuola (Medium seismicity site)						
	EFB		Uplift		Unstable	
	[-]	[%]	[-]	[%]	[-]	[%]
No-isol	1067	35.6	2084	69.5	1551	51.7
Isol-1	0	0.0	6	0.2	0	0.0
Isol-2	0	0.0	6	0.2	0	0.0
Isol-3	0	0.0	6	0.2	0	0.0
Isol-4	0	0.0	137	4.6	0	0.0
Isol-5	0	0.0	422	14.1	0	0.0
Isol-6	0	0.0	1713	57.1	370	12.3
Isol-7	0	0.0	1007	33.6	18	0.6
Isol-8	0	0.0	1469	49.0	17	0.6
Isol-9	0	0.0	2104	70.1	1114	37.1
Vibo Valentia (High seismicity site)						
	EFB		Uplift		Unstable	
	[-]	[%]	[-]	[%]	[-]	[%]
No-isol	1760	58.7	2582	86.1	2182	72.7
Isol-1	144	4.8	656	21.9	305	10.2
Isol-2	144	4.8	657	21.9	305	10.2
Isol-3	145	4.8	656	21.9	305	10.2
Isol-4	98	3.3	856	28.5	321	10.7
Isol-5	98	3.3	857	28.6	321	10.7
Isol-6	97	3.2	1654	55.1	368	12.3
Isol-7	104	3.5	1430	47.7	471	15.7
Isol-8	105	3.5	1616	53.9	469	15.6
Isol-9	103	3.4	2604	86.8	1164	38.8

In summary, the comparisons reveal that base shear is significantly reduced when tanks are isolated through CSS with different friction materials ("Isol-1÷9") compared to "fixed-base" tanks ("No-Isol"). Reductions range from -40% to -95%, with higher breakaway friction (μ_B) generally leading to increased base shear. In low seismicity zones, the reduction in base shear is less significant, averaging about -20% for "Isol-6" and "Isol-9," which have very high breakaway friction coefficients ($\mu_B=0.12$ and $\mu_B=0.20$, respectively).

Furthermore, J-factor analyses were conducted to assess partial base uplift and overall tank instability (overturning). Figure 5b shows median, 25th, and 75th percentile values of the J-factor calculated for seismic scenarios with a return period of 975 years (Life Safety Limit State) for medium seismicity sites. "Fixed-base" tanks ("No-Isol") consistently experience both uplift and overturning issues under all seismic scenarios. Isolated layouts ("Isol-1÷9") offer varying degrees of protection against these issues depending on the breakaway friction (μ_B). On average, uplift and instability thresholds are more frequently exceeded with increasing μ_B , especially in layouts with medium and high breakaway levels ("Isol-6÷9"). "Isol-9," for instance, is predicted to exceed both uplift and overturning thresholds in the medium seismicity site of Fiorenzuola. In contrast, "Isol-1-5" provide satisfactory performance against both uplift and overturning.

A total of 90,000 nonlinear dynamic analyses were conducted, and the results were grouped based on the seismicity level of the site (each including ten return periods) and the isolation system layout ("Isol-1÷9" and "No-isol"). Each group comprised 3,000 analyses (ten tanks, ten return periods, and 30 ground motions). The number of failures within each data group is shown in Table 2, with graphical representations in Figure 6 with regard to medium seismicity site.

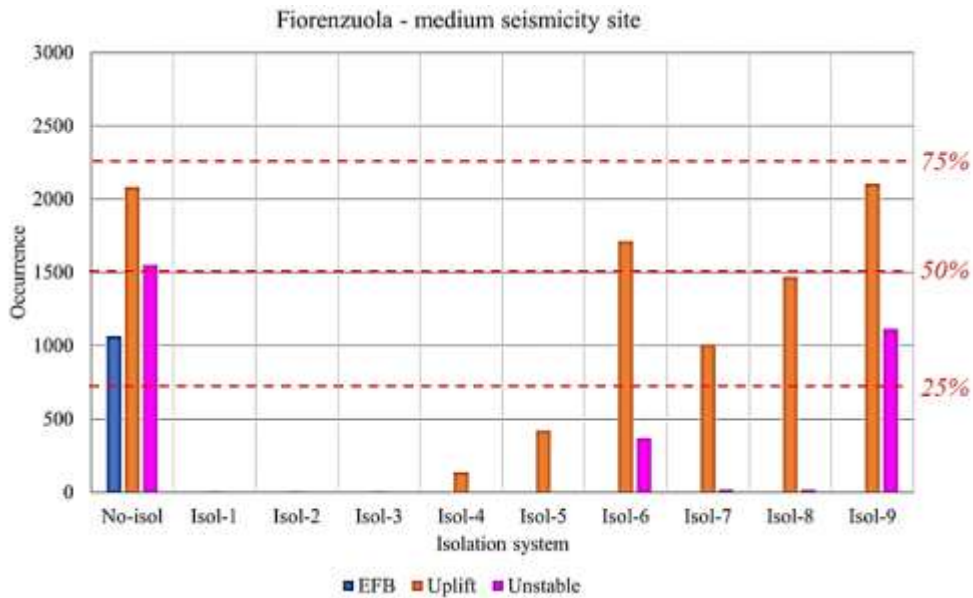


Figure 6 Occurrences of EFB, uplift and instability for site of Firenze (medium seismicity) (Gabbianelli et al., 2023)

It's important to note that due to the MSA approach and ground motion definitions, a direct comparison of "isolated tanks" in different sites based on their "average performances" is not straightforward. For example, the occurrence of EFB in "Isol-9" is higher for the low seismicity site of Sannazzaro compared to Firenze, despite the latter's higher seismicity. However, compared to "fixed-base" tanks ("No-isol"), all isolation layouts ("Isol-1÷9") significantly reduce, and in many cases, completely overcome the EFB issue regardless of the site's seismicity level (low, medium, or high).

Based on their performance against the risk of tank uplift and overturning, CSS isolators can be categorized into three groups. The first group includes CSS isolators with the highest breakaway friction, "Isol-9" ($\mu_B=0.20$), offer limited protection against uplift at all seismicity levels (occurrences > 50%) and are comparable to "fixed-base" tanks. Their stability against overturning is also concerning, with occurrences ranging from 30% to 40%. The second group consists of CSS isolators with medium-high breakaway friction, "Isol-6÷8" ($\mu_B=0.05\div0.12$), provide moderate protection against uplift (occurrence range 32÷57%) but offer better performance against tank overturning (occurrence < 20%). The latter group is formed by CSS isolators with low breakaway friction, "Isol-1÷5" ($\mu_B=0.01\div0.06$), are predicted to offer good protection against uplift (occurrence < 20%) and complete protection against overturning (occurrence = 0%) at low and medium seismicity levels. For the strongest seismic scenario (Vibo Valentia), their effectiveness slightly decreases, with maximum failure percentages of 29% and 11% for uplift and overturning, respectively.

These results demonstrate that the proper selection of CSS isolators can significantly reduce or eliminate the risk of both tank uplift and overturning, with further technical details to be defined for project-specific requirements.

Finally, the performed analysis have also been used to define the fragility curves associated to every case as reported by Gandelli et al. (2022).

5. Conclusions and future developments

Recent research has demonstrated the effectiveness of Curved Surface Sliders (CSS) for seismic protection of steel storage tanks. However, little attention has been given to potential issues related to the peak friction force at CSS motion breakaway due to limited formulations in commercial Finite Element Method (FEM) codes. To address this, in the present study which included some findings discussed by Gabbianelli et al. (2023) an advanced model in the OpenSees FEM code has been developed to simulate the seismic response of isolated tanks, accounting for the breakaway effect.

A comprehensive parametric study was conducted to investigate the impact of varying "breakaway friction" levels ($\mu_B=0.01\div 0.20$) on critical aspects affecting tank seismic response, including "elephant foot buckling" (EFB), uplift, and overturning. The findings from nonlinear time-history analyses (NLTH) reveal that all isolation configurations offer excellent protection against EFB. However, the results highlight that CSS isolators with very high breakaway friction, like "Isol-9" ($\mu_B=0.20$), provide limited protection against uplift, with nearly 90% failure rates during intense seismic events. Their response is akin to that of traditional "fixed-base" tanks, offering no substantial advantage. Additionally, the tanks' stability against overturning is not reassuring, with failure percentages ranging from 30% to 40% at all seismicity levels. Furthermore, CSS isolators with medium-high breakaway friction, such as "Isol-6÷8" ($\mu_B=0.05\div 0.12$), still exhibit limited protection against uplift, with predicted failure rates ranging from 30% to 60% at all seismicity levels. However, these devices demonstrate improved performance in terms of preventing tank overturning, with failure rates below 20%. Finally, CSS isolators with low breakaway friction, such as "Isol-1÷5" ($\mu_B=0.01\div 0.06$), offer excellent protection against both uplift and overturning during low to medium-intensity seismic events, with expected failure rates below 20% and 0%, respectively. Even during very strong earthquakes, their effectiveness only slightly diminishes, with maximum failure rates reaching about 30% for uplift and 10% for overturning.

While further investigations are warranted, including the consideration of CSS with varying radius of curvature and different foundation soil categories, it can be concluded that CSS isolators with low breakaway friction are the preferred choice for seismic protection of steel storage tanks. They have the potential to significantly mitigate or even eliminate both uplift and overturning issues. The analyses performed have permitted the definition of fragility curves (Gandelli et al., 2022).

6. Acknowledgements

The authors gratefully acknowledge the Italian Department of Civil Protection (DPC) for their financial contributions to this study through the 2022-2023 Project (Work Package 15).

7. References

- API Standard 650. (2020). *Welded tanks for oil storage*, American Petroleum Institute, API Publishing Services, Washington D.C..
- Bakalis, K., Karamanos, S.A., (2021). Uplift Mechanics of Unanchored Liquid Storage Tanks Subjected to Lateral Earthquake Loading. *Thin-Walled Structures*. <https://doi.org/10.1016/j.tws.2020.107145>.
- Baker, J. W. (2015). Efficient Analytical Fragility Function Fitting Using Dynamic Structural Analysis. *Earthquake Spectra*. <https://doi.org/10.1193/021113EQS025M>.
- Brunesi, E., Nascimbene, R., Pagani, M., Bellic, D., (2015). Seismic Performance of Storage Steel Tanks during the May 2012 Emilia, Italy, Earthquakes. *Journal of Performance of Constructed Facilities*. [https://doi.org/10.1061/\(asce\)cf.1943-5509.0000628](https://doi.org/10.1061/(asce)cf.1943-5509.0000628).
- Caprinuzzi, S., Paolacci, F., Dolšek, M., (2020). Seismic Risk Assessment of Liquid Overtopping in a Steel Storage Tank Equipped with a Single Deck Floating Roof. *Journal of Loss Prevention in the Process Industries*. <https://doi.org/10.1016/j.jlp.2020.104269>.
- Cardone, D., Gesualdi, G., Brancato, P., (2015). Restoring capability of friction pendulum seismic isolation systems. *Bulletin of Earthquake Engineering* 13(8). doi: 10.1007/s10518-014-9719-5.
- Constantinou, M.C., Mokha, A., Reinhorn, A. (1990). Teflon bearings in base isolation II: modeling. *Journal of Structural Engineering ASCE*. 116(2): 455-474, doi: 10.1061/(ASCE)0733-9445(1990)116:2(455)
- Cornell, C.A. (1968). Engineering Seismic Risk Analysis. *Bulletin of the Seismological Society of America* 58 (5): 1583–1606.

- EN 1998-1. (2011). *Eurocode 8: Design of Structures for Earthquake Resistance - Part 1: General Rules, Seismic Actions and Rules for Buildings*. European Committee for Standardisation, Brussels, Belgium.
- EN 1998-4. (2006). *Eurocode 8: Design of Structures for Earthquake Resistance - Part 4: Silos, Tanks and Pipelines*. European Committee for Standardisation, Brussels, Belgium.
- Gabbianelli, G., Milanesi, R.R., Gandelli, E., Dubini, P., Nascimbene, R., (2023). Seismic vulnerability assessment of steel storage tanks protected through sliding isolators. *Earthquake Engineering & Structural Dynamics*, 52(9), pp.2597-2618.
- Gandelli, E., Penati, M., Quaglini, V., Lomiento, G., Miglio, E., Benzoni, G. M. (2019). A novel OpenSees element for single curved surface sliding isolators. *Soil Dynamics and Earthquake Engineering* 119. <https://doi.org/10.1016/j.soildyn.2018.01.044>
- Gandelli, E., Quaglini V., (2020) Effect of the static coefficient of friction of curved surface sliders on the response of an isolated building. *Journal of Earthquake Engineering* 24(9). Taylor & Francis, <https://doi.org/10.1080/13632469.2018.1467353>
- Gandelli, E., De Domenico, D., Dubini, P., Besio, M., Quaglini V., (2020). Influence of the breakaway friction on the seismic response of buildings isolated with curved surface sliders: Parametric study and design recommendations. *Structures* 27, Elsevier, <https://doi.org/10.1016/j.istruc.2020.06.035>
- Gandelli, E., Gabbianelli, G., Milanesi R.R., Dubini, P., Nascimbene, R., Pavese, A., (2022). Refined numerical modelling of steel storage tanks implementing sliding isolators, *Proc. 2nd Euroasian Opensees Days Conference (EOSD 2022)*, 7-8 July 2022, Turin, Italy.
- Malhotra, P.K. (1997). Seismic Response of Soil-Supported Unanchored Liquid-Storage Tanks. *Journal of Structural Engineering*. [https://doi.org/10.1061/\(asce\)0733-9445\(1997\)123:4\(440\)](https://doi.org/10.1061/(asce)0733-9445(1997)123:4(440)).
- Malhotra, P.K. (2000). Practical Nonlinear Seismic Analysis of Tanks. *Earthquake Spectra*. <https://doi.org/10.1193/1.1586122>.
- McKenna, F., Fenves, G., Scott, M., (2006). *Computer program OpenSees: open system for earthquake engineering simulation*. <https://opensees.berkeley.edu>
- Merino Vela, R. J., Brunesi, E., Nascimbene, R., (2018). Derivation of Floor Acceleration Spectra for an Industrial Liquid Tank Supporting Structure with Braced Frame Systems. *Engineering Structures*. <https://doi.org/10.1016/j.engstruct.2018.05.053>.
- Merino Vela, R.J., Brunesi, E., Nascimbene, R., (2019). Floor Spectra Estimates for an Industrial Special Concentrically Braced Frame Structure. *Journal of Pressure Vessel Technology*, Transactions of the ASME. <https://doi.org/10.1115/1.4041285>.
- Naeim, F., Kelly, J.M., (1999). *Design of Seismic Isolated Structures: From Theory to Practice*. John Wiley & Sons. New York.
- NTC18. (2018). *Norme Tecniche per Le Costruzioni. DM 17/1/2018*. [in Italian] Gazzetta Ufficiale della Repubblica Italiana, Italian Ministry of Infrastructure and Transport, Rome, Italy.
- Pavese, A., Furinghetti, M., Casarotti, C., (2019). Investigation of the consequences of mounting laying defects for curved surface slider devices under general seismic input. *Journal of Earthquake Engineering* 23(3). <https://doi.org/10.1080/13632469.2017.1323046>
- Quaglini, V., Dubini, P., Poggi, C., (2012). Experimental assessment of sliding materials for seismic isolation systems. *Bulletin of Earthquake Engineering* 10(2). doi: 10.1007/s10518-011-9308-9.
- Quaglini, V., Gandelli, E., Dubini, P., (2019). Numerical investigation of curved surface sliders under bidirectional orbits, *Ingegneria Sismica - International Journal of Earthquake Engineering*. 2019(2), Patron editore
- Takashi, N., (1994). ALE Finite Element Computations of Fluid-Structure Interaction Problems. *Computer Methods in Applied Mechanics and Engineering* 112 (1–4). [https://doi.org/10.1016/0045-7825\(94\)90031-0](https://doi.org/10.1016/0045-7825(94)90031-0).